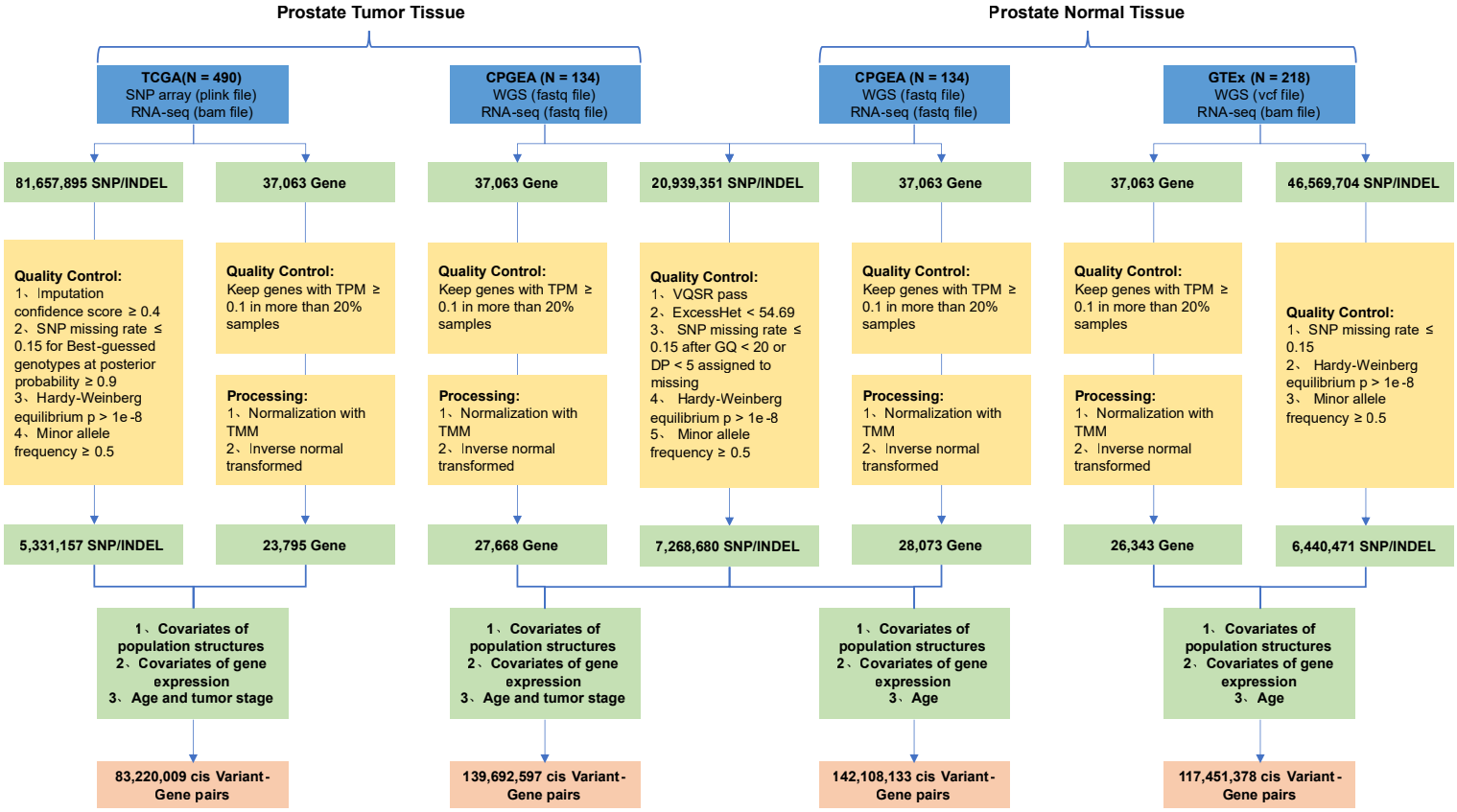

Supplementary Fig. 1. Overview of the cis-eQTL analysis pipeline in CPGEA, GTEx, and TCGA. The upper section of the flowchart outlines the number of samples, initial variants, and genes included from the CPGEA, GTEx, and TCGA datasets. The middle section details the consistent quality control measures and preprocessing applied to the variants and genes. The bottom section illustrates the cis-eQTL analysis performed on the quality-controlled variants and genes, specifying the covariates used for analyses in normal and tumor samples. The resulting cis variant-gene pair associations were utilized in this study.

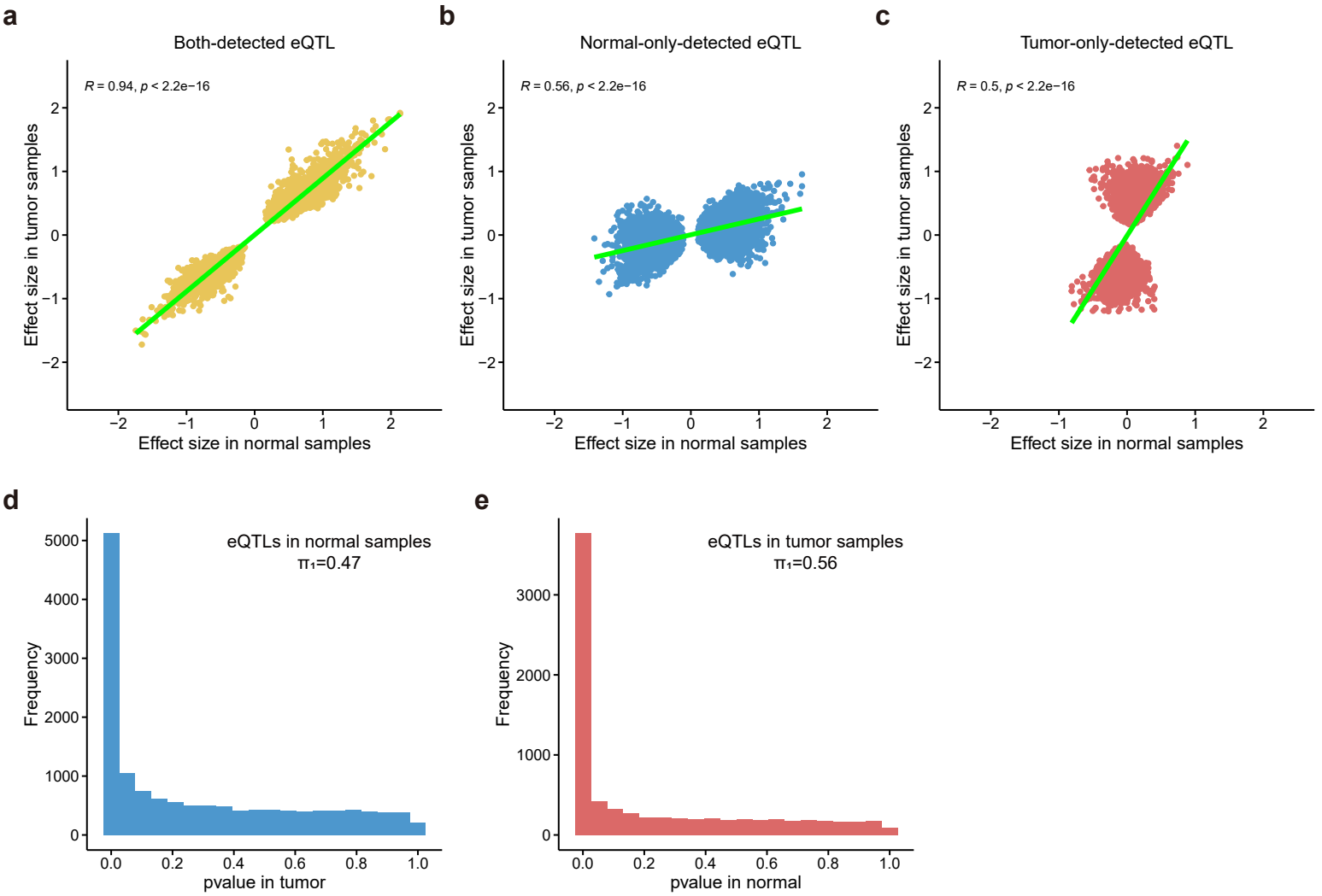

Supplementary Fig. 2. Correlation of effect sizes between normal and tumor samples.
(a-c) Scatter charts depicting the correlation of effect sizes between normal and tumor samples for both-detected (a), normal-only-detected (b), and tumor-only-detected (c) eQTLs. Spearman correlation analysis was performed to assess the relationships. (d) *P*-value distributions and statistical comparisons of normal-only-detected and both-detected eQTLs in tumor eQTL analysis. (e) *P*-value distributions and statistical comparisons of tumor-only-detected and both-detected eQTLs in normal eQTL analysis.

Xu *et al*. Supplementary Fig. 3

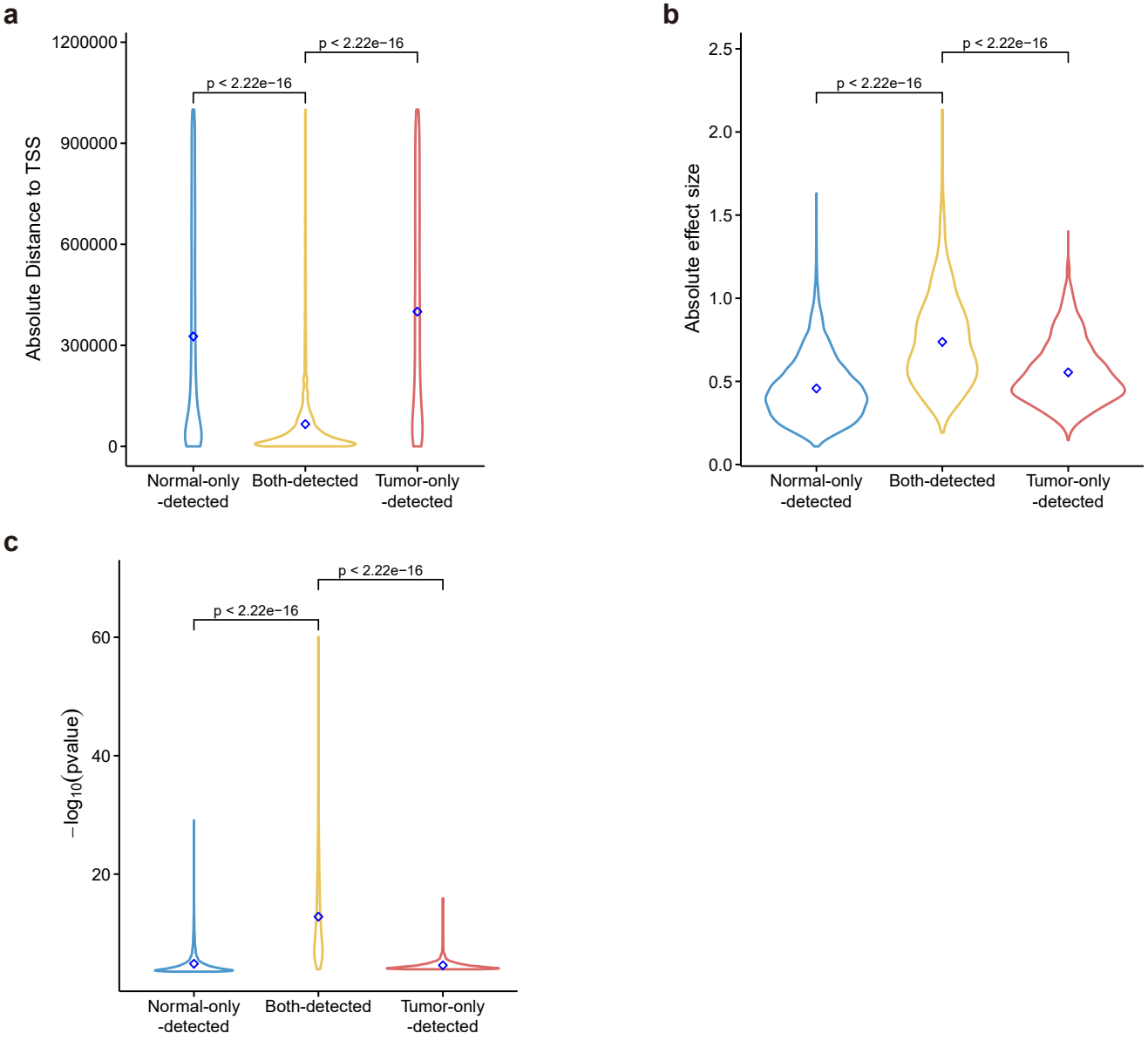

Supplementary Fig. 3. Comparison of three groups of eQTL.
(a-c) Violin plots comparing the absolute distance to the transcription start site (TSS) (a), absolute effect size (b), and -log10(P-value) (c) among both-detected eQTLs, normal-only-detected eQTLs, and tumor-only-detected eQTLs. *P*-values were calculated using the Wilcoxon rank sum test.

Xu *et al*. Supplementary Fig. 4

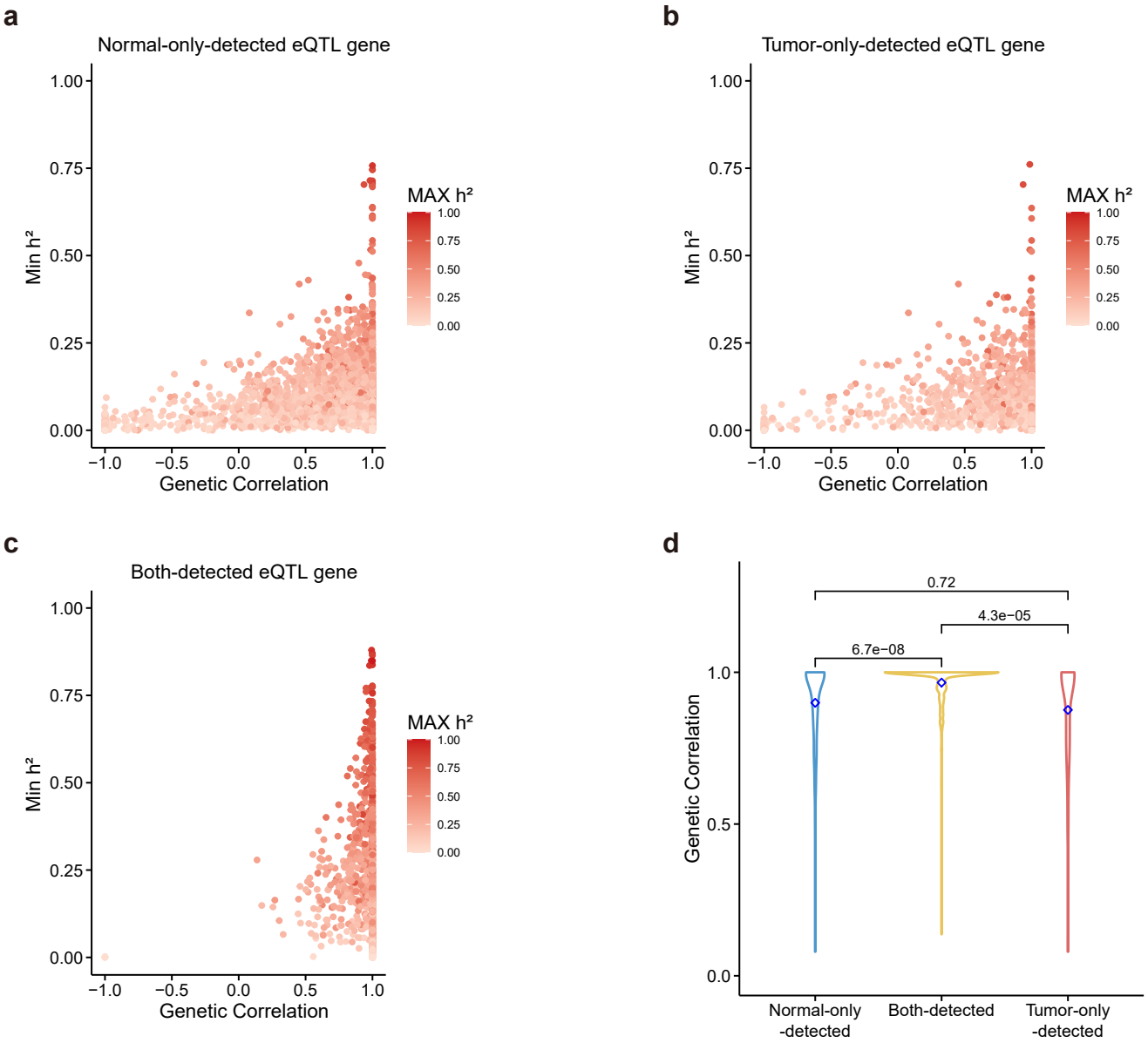

Supplementary Fig. 4. Comparisons and distributions of genetic correlations.
(a-c) Scatter charts illustrating the distribution of genetic correlations for normal-only-detected eQTL-genes (eGenes) (a), tumor-only-detected eGenes (b), and both-detected eGenes (c). The x-axis represents the smallest heritability of each gene, while the color gradient indicates the largest heritability, ranging from 0 to 1. (d) Genetic correlations between normal and tumor samples for normal-only-detected, tumor-only-detected, and both-detected eGenes. *P*-values were calculated using the Wilcoxon rank sum test.

Xu *et al*. Supplementary Fig. 5

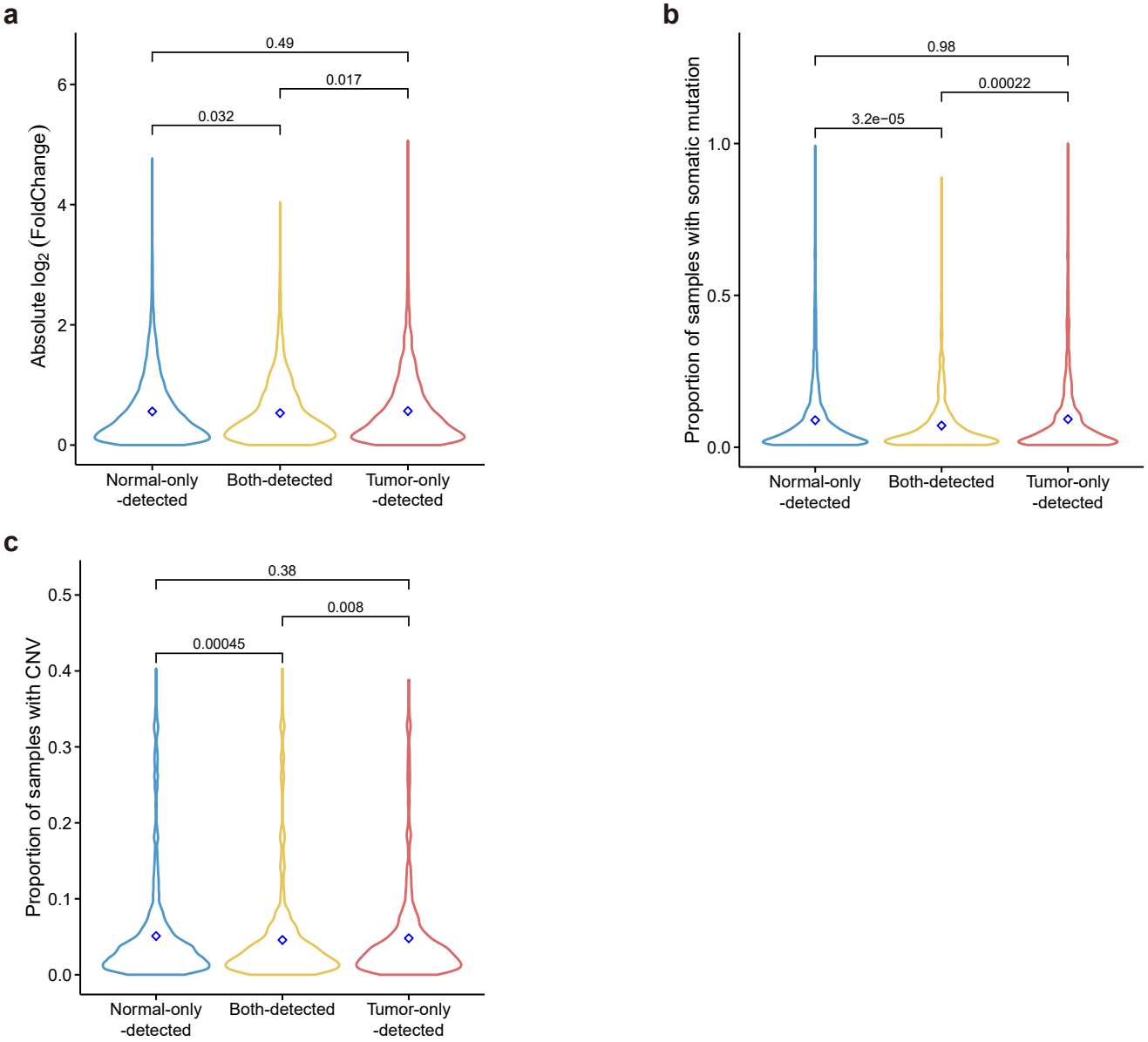

Supplementary Fig. 5. Comparisons of three groups of eQTL genes.
(a) Absolute log2(fold change) of normal-only-detected, tumor-only-detected, and both-detected eQTL-associated genes (eGenes) between normal and tumor samples. (b-c) Proportions of samples with somatic mutations (b) or copy number variations (CNVs) (c) in normal-only-detected, tumor-only-detected, and both-detected eGenes. *P*-values were calculated using the Wilcoxon rank sum test.

Xu *et al*. Supplementary Fig. 6

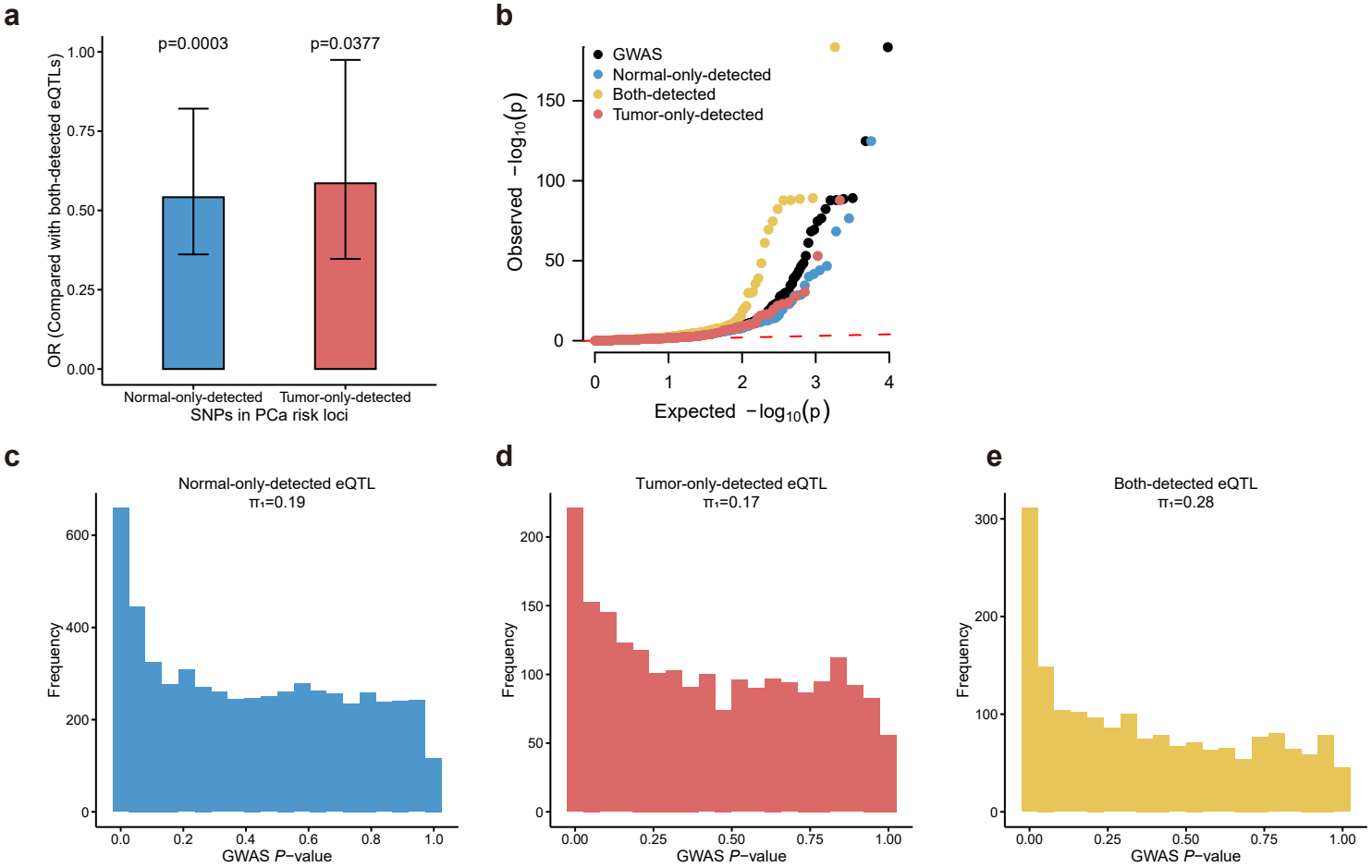

Supplementary Fig. 6. GWAS SNPs enrichment comparison of three groups of eQTL.
(a) Odds ratios (ORs) from enrichment analysis of normal-only-detected and tumor-only-detected eQTLs among PCa risk loci compared with both-detected eQTLs. Significant GWAS SNPs (*P*-value < 5e-8) were obtained from GWAS summary data of GWAS catalog (Study Accession for the GWAS summary data: GCST90274713). (b) Quantile–quantile plots displaying normal-only-detected, tumor-only-detected, both-detected eQTLs, and genome-wide SNPs from the same GWAS summary data. GWAS SNPs are annotated based on their overlap with normal-only-detected, tumor-only-detected and both-detected eQTLs. (c-e) GWAS *P*-value distributions and statistical comparisons for normal-only-detected (c), tumor-only-detected (d), and both-detected (e) eQTLs.

Xu *et al*. Supplementary Fig. 7

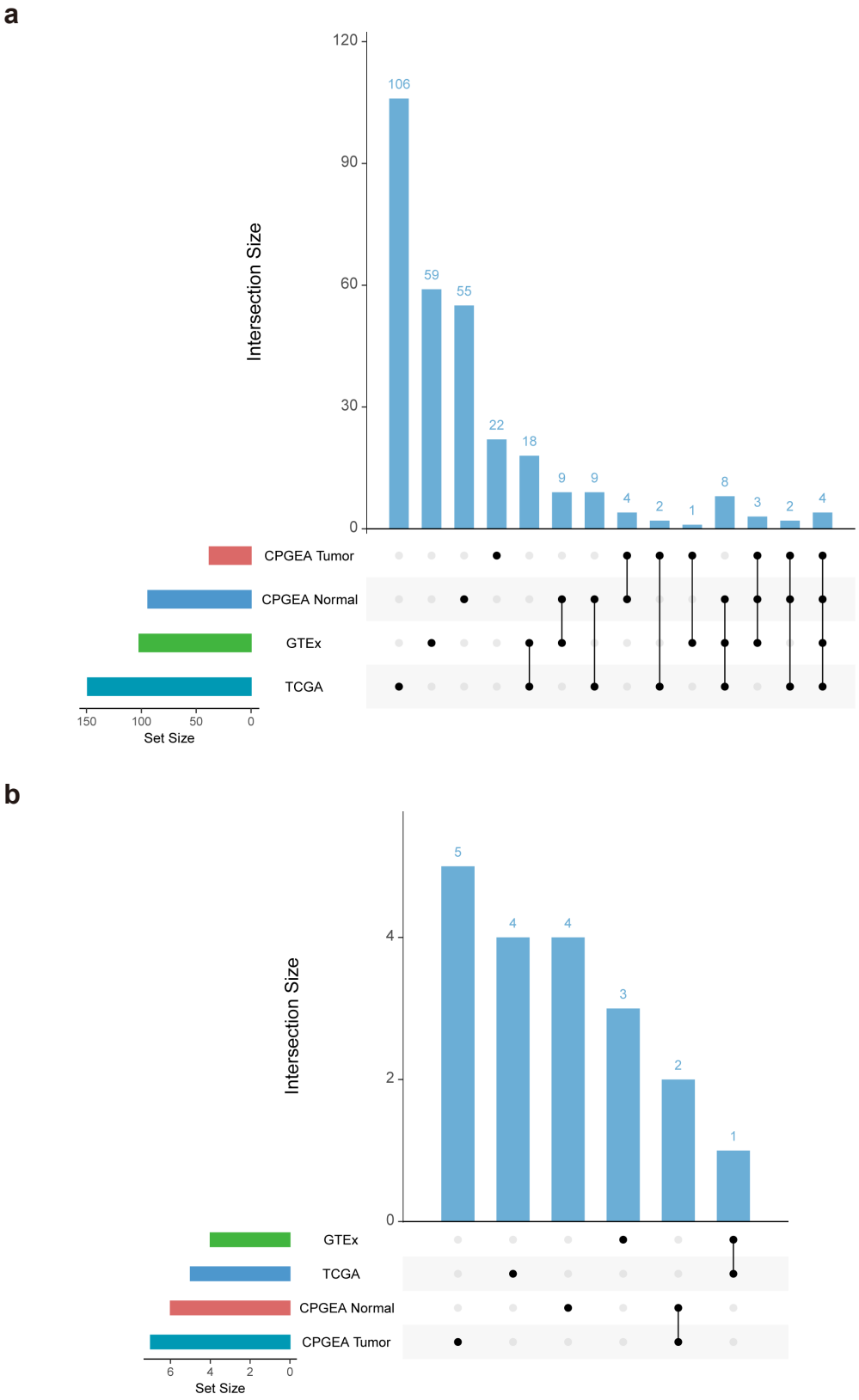

Supplementary Fig. 7. Colocalization results using GWAS summary data from EUR and EAS populations. (a-b) Upset plots showing the number of colocalized genes identified in CPGEA Normal, CPGEA Tumor, GTEx, and TCGA datasets for EUR (a) and EAS (b) populations. The plots display the number of genes unique to each dataset and those shared across multiple datasets.

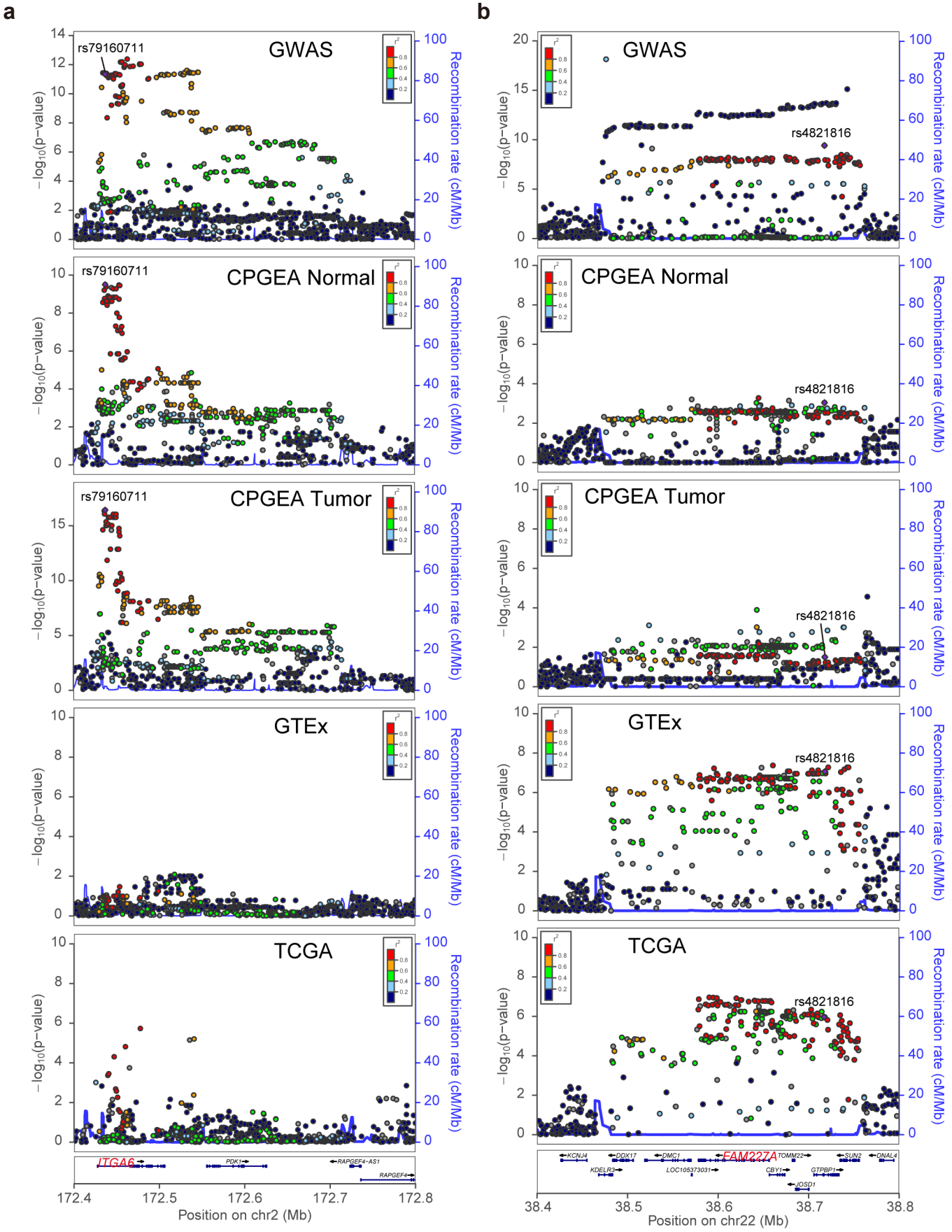

Supplementary Fig. 8. LocusZoom plot for *ITGA6* and *FAM227A*.
(a-b) LocusZoom plots illustrating the *P*-value and linkage disequilibrium (LD) distribution of GWAS SNPs and eQTLs from CPGEA Normal, CPGEA Tumor, GTEx, and TCGA datasets. The plots display upstream and downstream regions of *ITGA6* (a) and *FAM227A* (b) in a top-to-bottom arrangement.

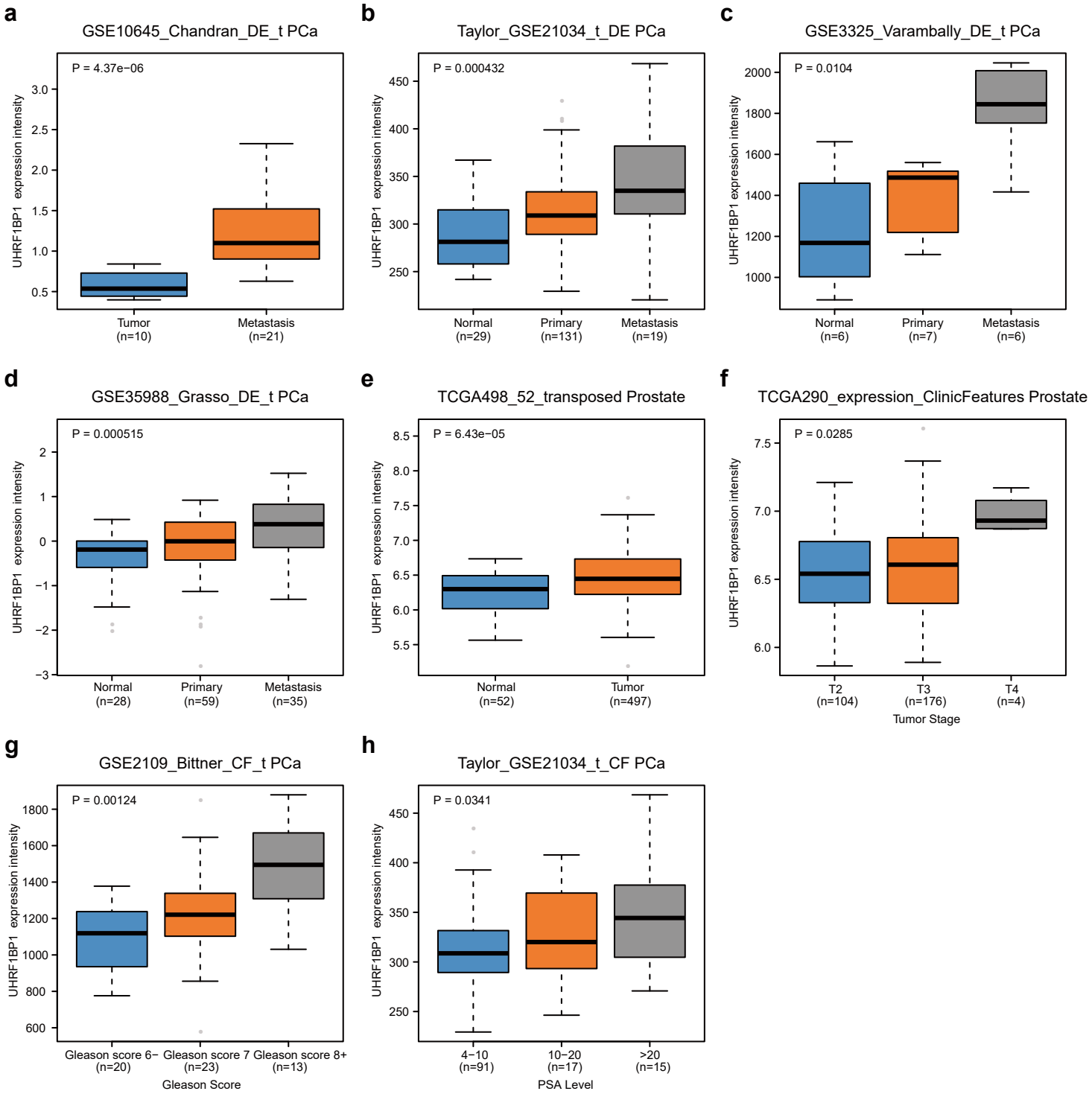

Supplementary Fig. 9. Clinical analysis of UHRF1BP1 expression.
(a-e) Comparison of UHRF1BP1 expression levels among normal, primary tumor, and metastasis tumor samples in GSE10645 (a), GSE21034 (b), GSE3325 (c), GSE35988 (d), and TCGA (e). Results indicate significantly higher expression of UHRF1BP1 in tumor and metastatic samples. (f-h) Comparison of UHRF1BP1 expression across clinical subgroups based on tumor stage (f), Gleason score (g) and PSA level (h). UHRF1BP1 expression is significantly elevated in samples with higher Gleason scores, elevated PSA levels, and advanced tumor stages. All *P*-values were calculated using the Kruskal-Wallis test.

Xu *et al*. Supplementary Fig. 10

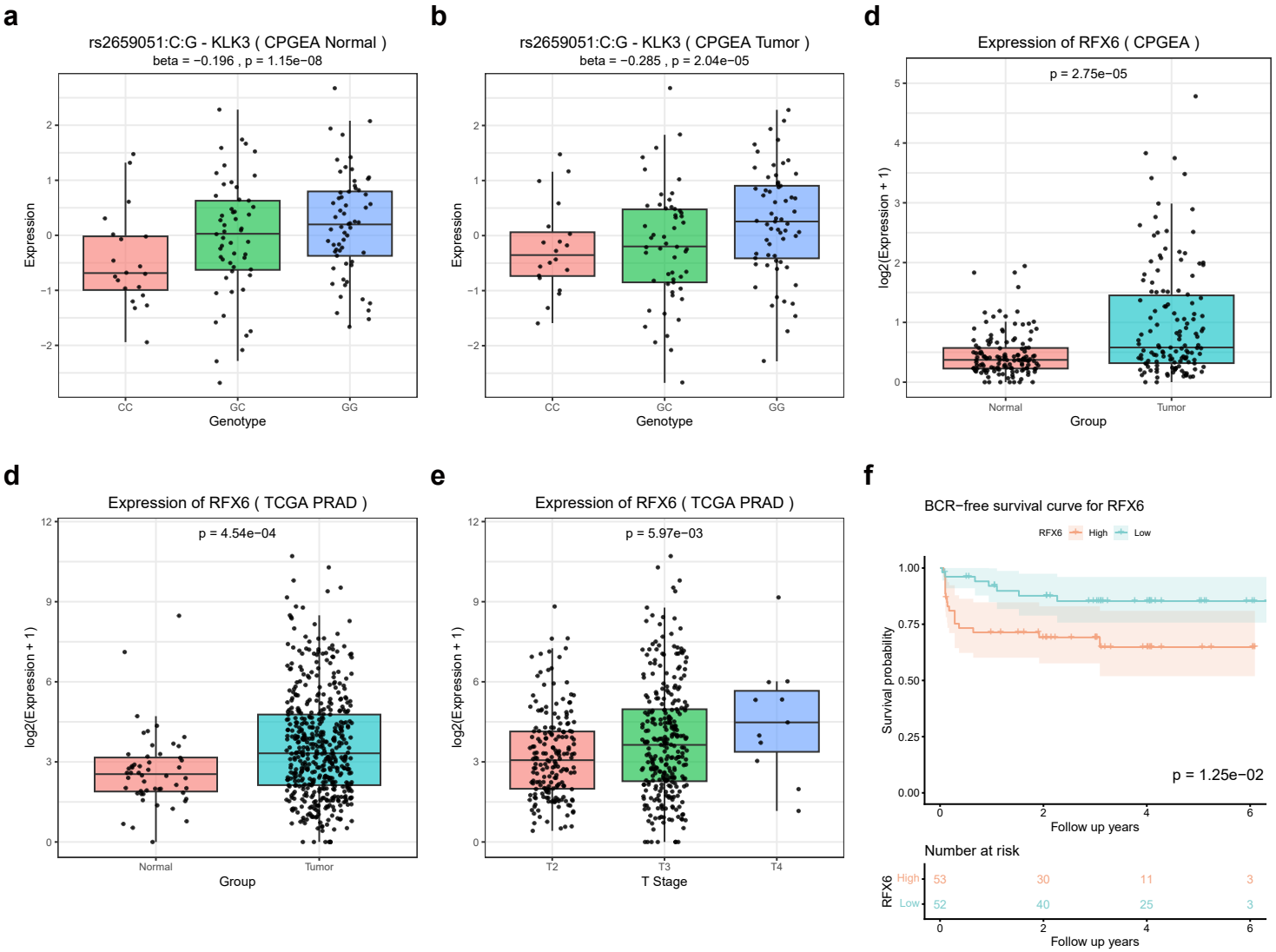

Supplementary Fig. 10. Examples of plots downloaded from ProstateOmicsQTLAtlas.
(a-b) The eQTL results showing the G allele of rs2659051 was associated with the high expression of KLK3 in CPGEA Normal (a) and CPGEA Tumor (b).(c-d) Boxplot showing expression of RFX6 was higher in tumor samples than in normal samples in CPGEA (c) and TCGA (d). (e) Expression of RFX6 was positively correlated with tumor satge in TCGA. (f) Samples with higher expression of RFX6 showing poor prognosis in DFKZ.

Xu *et al*. Supplementary Fig. 11

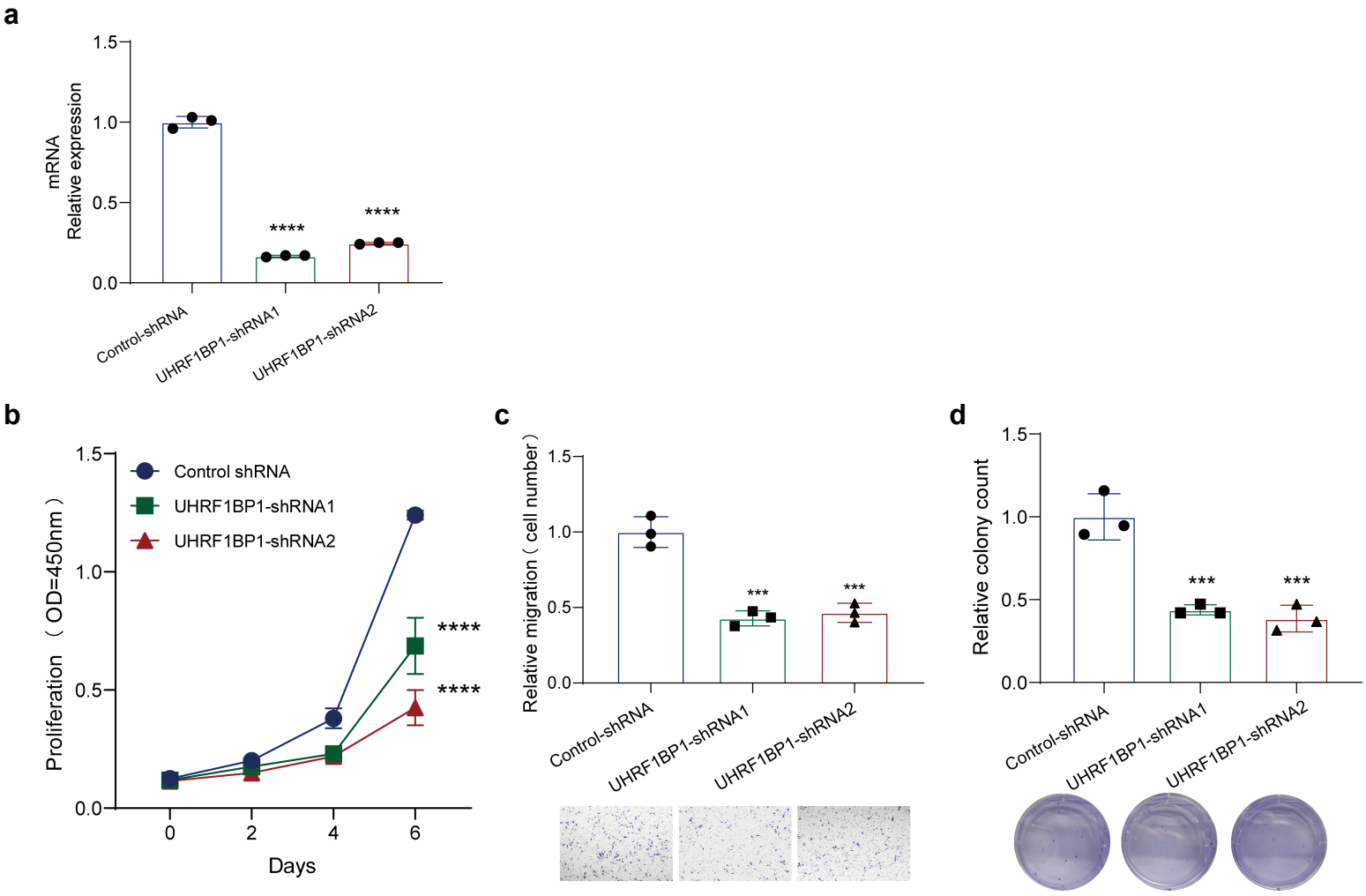

Supplementary Fig. 11. Functional roles of UHRF1BP1 in C4-2 prostate cancer cells.
(a) Quantitative RT-PCR analysis of the mRNA levels of UHRF1BP1 in C4-2 with different shRNAs. Error bars, ± SD from three technical replication. (c-d) UHRF1BP1 promotes PCa cell proliferation, as demonstrated by MTT assays (b), migration assays (c), and colony formation assays (d), with results presented as mean ± SEM from triplicate experiments. Experiments were conducted in C4-2 cells transduced with gene-specific or control shRNAs. Statistical significance was assessed using two-tailed Student's t tests, with significance levels indicated as *p < 0.05, **p < 0.01, ***p < 0.001, and ****p < 0.0001.

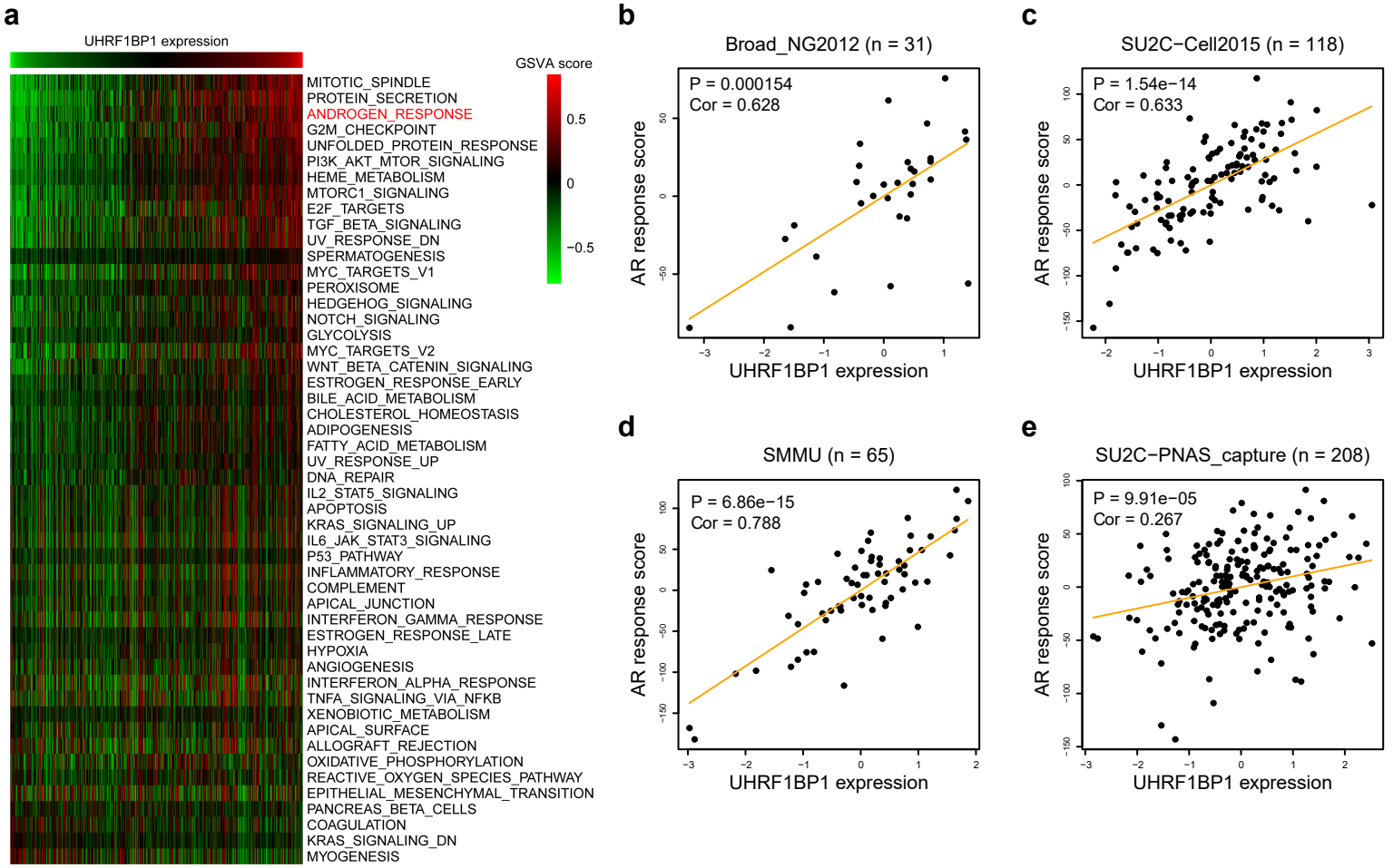

Supplementary Fig. 12. Correlation between the androgen response pathway and UHRF1BP1 expression. (a) Heatmap displaying GSVA scores for Hallmark pathways across TCGA samples, arranging from low (left) to high (right) based on UHRF1BP1 expression. Hallmark pathways are ranked from high (top) to low (bottom) according to their correlations with UHRF1BP1 expression. (b-e) Scatter plots showing the correlation of between UHRF1BP1 expression and androgen response scores in the Broad (b), U2C-Cell (c), SMMU (d), and SU2C-PNAS (e). Spearman's rank correlation analysis was used to calculate the correlations.

Xu *et al*. Supplementary Fig. 13

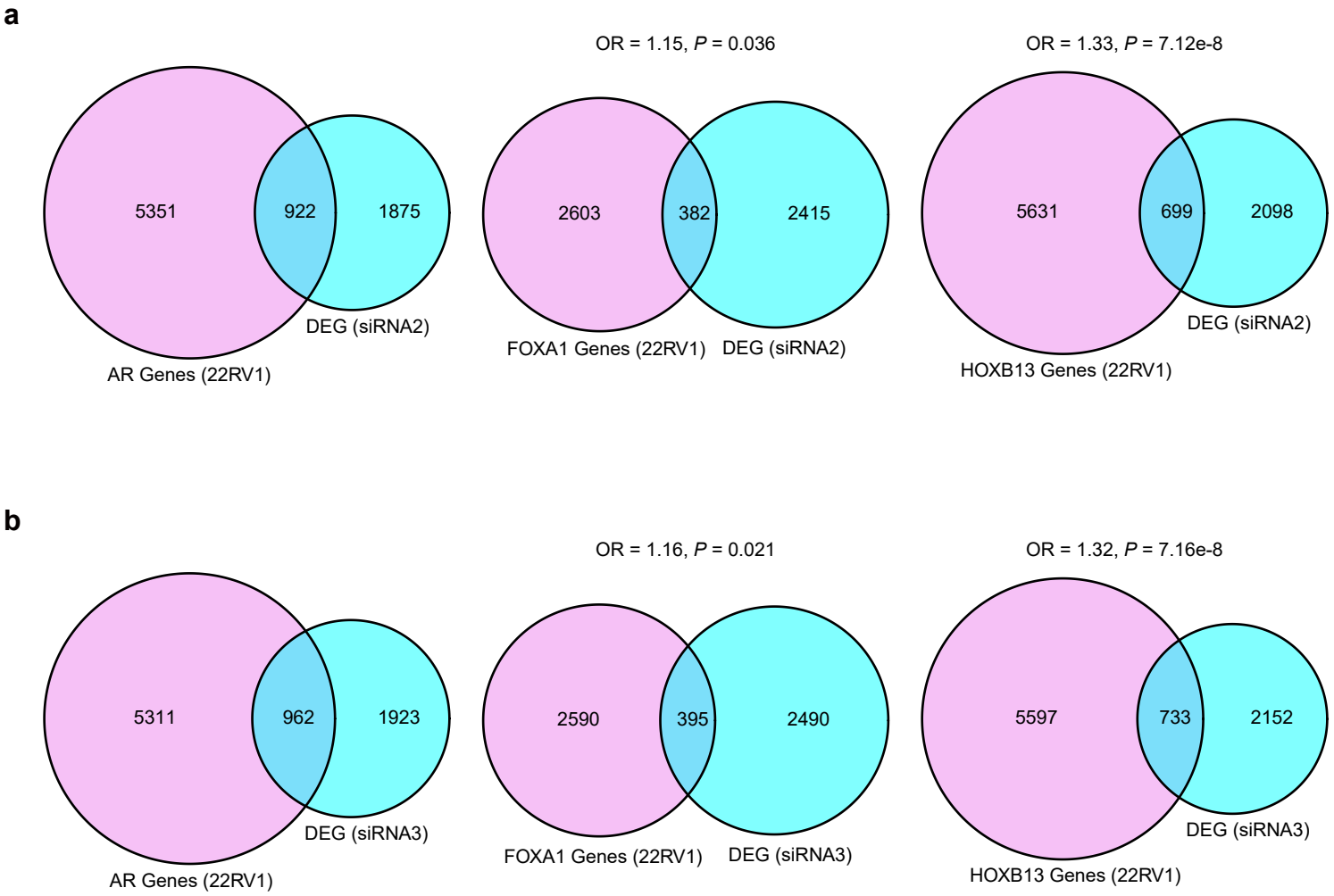

Supplementary Fig. 13. Overlap between transcription factor binding genes and differentially expressed genes (DEGs) following UHRF1BP1 knockdown.
(a-b) Overlap analysis of AR, FOXA1, and HOXB13 binding genes with DEGs identified after UHRF1BP1 knock-down using siRNA1 (a) or siRNA2 (b). Only genes annotated as promoter-TSS regions were considered as binding genes. The odds ratio (OR) and *P*-value compared to AR were calculated using Fisher's exact test. An OR > 1 indicates that DEGs were more enriched in AR binding genes.

Xu *et al*. Supplementary Fig. 14

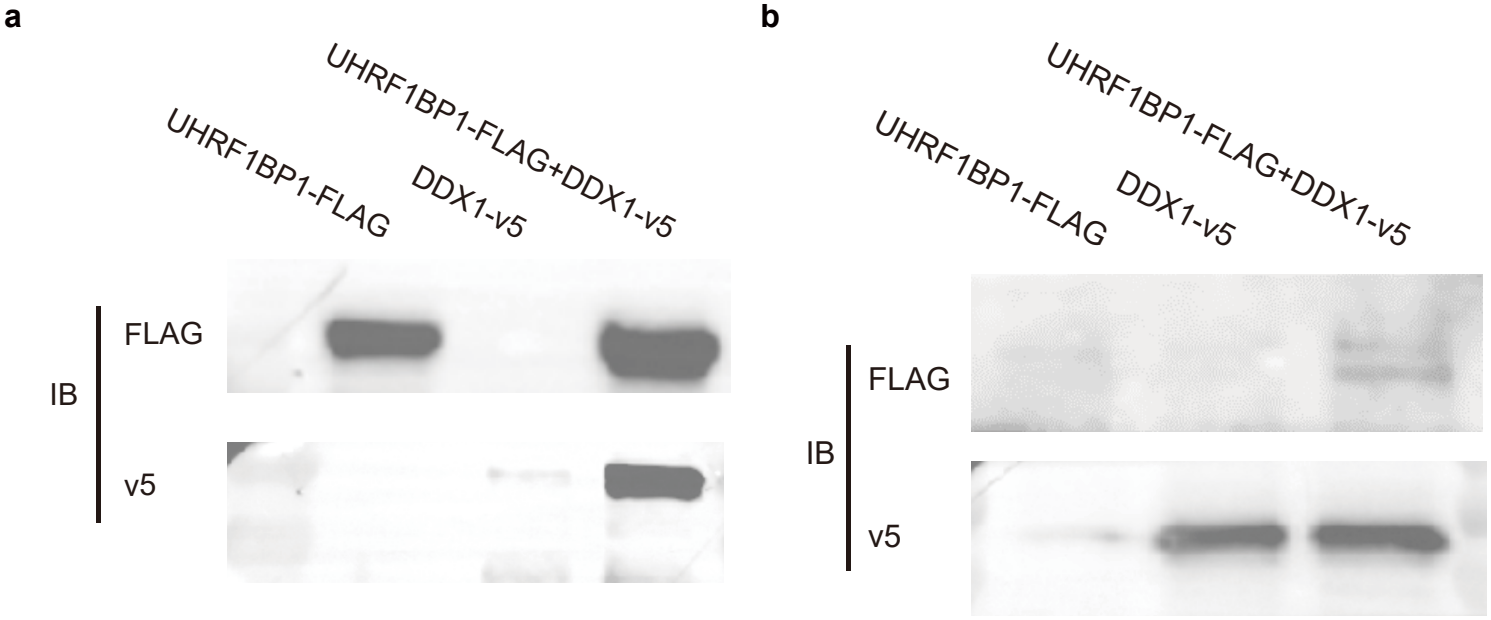

Supplementary Fig. 14. Co-immunoprecipitation (Co-IP) experiments between UHRF1BP1 and DDX1 in the 293T cell line.
(a) Co-IP assays were performed after transfecting 293T cells with plasmids encoding DDX1-V5, UHRF1BP1-FLAG, or co-transfecting both plasmids. (b) Immunoprecipitation was carried out using anti-FLAG or anti-V5 antibodies, followed by immunoblotting (IB) analysis to detect FLAG and V5-tagged proteins.

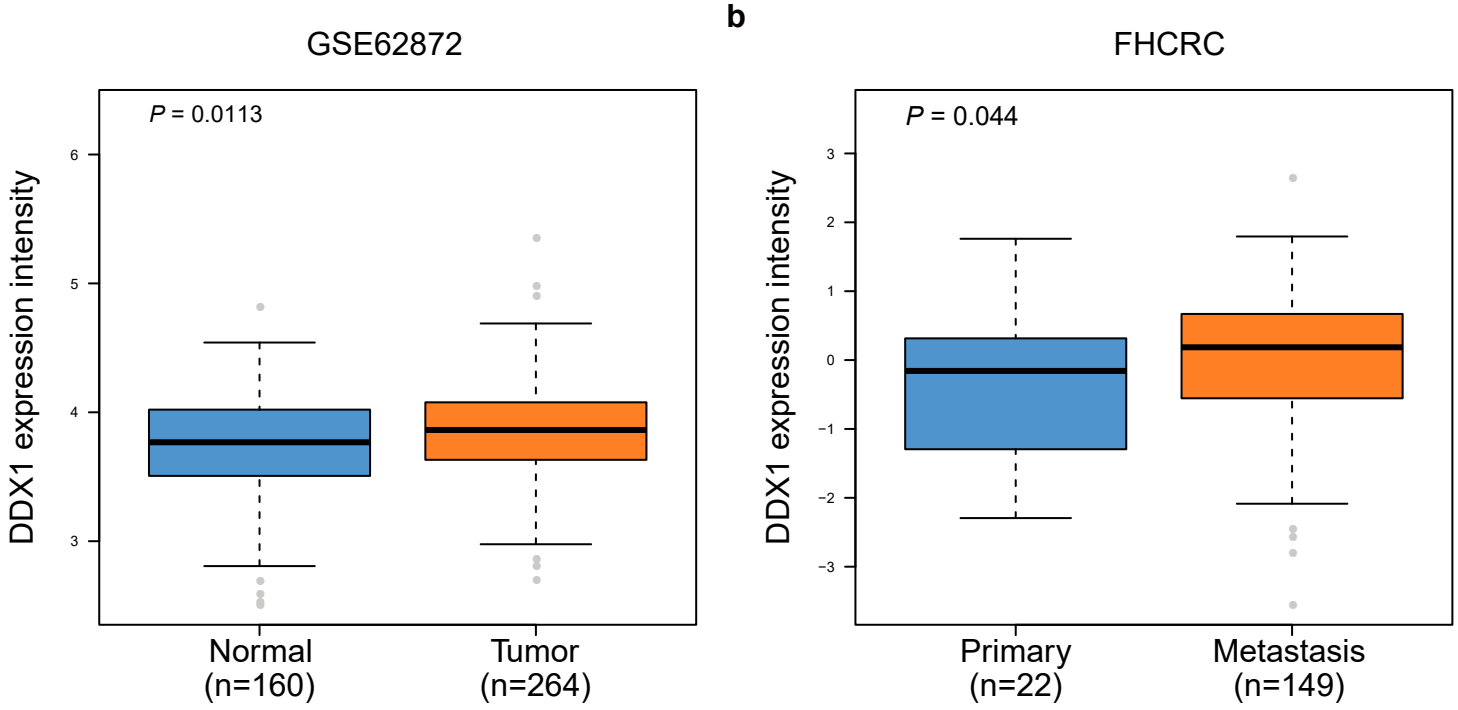

Supplementary Fig. 15. Differential expression of *DDX1*
(a) DDX1 gene was highly expressed in tumor samples compared to normal samples in GSE62872. (b) The high expression of DDX1 in metastatic samples was higher than that in primary tumor tissues in FHCRC.